16th Australasian Fluid Mechanics Conference
Crown Plaza, Gold Coast, Australia
2-7 December 2007

PIV Study of the Vortex Wake behind a Translationally Oscillating Cylinder in a Quiescent Fluid

M. Nazarinia, J. Sheridan, M.C. Thompson and J. Carberry

Department of Mechanical and Aerospace Engineering
Monash University, Melbourne, Victoria, 3800 AUSTRALIA

Abstract

The near wake produced by a circular cylinder oscillating translationally in a quiescent fluid or, alternatively, by oscillatory flow past a stationary cylinder at low Keulegan-Carpenter (KC) and Stokes (β) numbers has been investigated using Particle Image Velocimetry. All but one of the two- and three-dimensional regimes of the Tatsuno & Bearman [11] map were investigated. The findings are successfully compared with previous experimental observations and numerical simulations. Two-dimensional Particle Image Velocimetry results of regime B show how the symmetrical pattern of vortices around the cylinder becomes three-dimensional. Additionally, the instantaneous results of regime E confirm that there is an intermittent change in the direction of the V-shaped vortices around the cylinder.

Introduction

The study of the oscillating flow around circular cylinders is important in off-shore engineering because this flow is an idealized representation of the wave-induced loads on cylindrical structures, while oscillation of the cylinder in quiescent fluid, or the converse situation of oscillating flow past a stationary cylinder, are effective representations of wave-cylinder interaction in the area of the ocean engineering [8].

It is well known that when a bluff body is oscillated in a quiescent fluid, secondary streaming is generated around the body owing to the influence of nonlinear effects. On the other hand, when the amplitude of oscillation of a body or a flow is increased beyond a certain critical value, flow separation occurs on the body surface and vortices are formed in each half-cycle [2]. When the relative flow past a cylinder is undergoing sinusoidal oscillations the structure of the flow generated by the cylinder depends mainly on two parameters: the Keulegan-Carpenter number, KC, defined by

$$KC = \frac{U_{\max}}{f_t D} = \frac{2\pi A_t}{D}, \tag{1}$$

where $U_{\max}$ is the maximum velocity of the cylinder motion, f_t is the frequency of oscillation, D is the diameter of the cylinder and A_t is the amplitude of the relative motion; and the Stokes number, β, defined by

$$\beta = \frac{f_t D^2}{\nu}, \tag{2}$$

where ν the kinematic viscosity of the fluid. The associated Reynolds number, Re, is

$$Re = \frac{U_{\max} D}{\nu} = KC \cdot \beta. \tag{3}$$

In other words, KC and β are representative of dimensionless amplitude and frequency of oscillation, respectively.

The flow at very small KC has been studied analytically by Stokes [10] and then Wang [12], who developed an asymptotic theory assuming that the flow remains attached. Tatsuno & Bearman [11] took this work further and produced a control-space map, classifying the flows into eight flow regimes each with a two- and three-dimensional flow structure and vortex shedding characteristics. Using two different flow visualisation techniques, they comprehensively investigated translational harmonic oscillation in a quiescent fluid over a range of independent variables, e.g. the amplitude and frequency of oscillations corresponding to KC and β numbers, respectively. They have covered the range of KC between 1.6 and 15 and β between 5 and 160 but without quantitative measurements. A reduced version of the (KC-β)-space map they produced is shown in figure 1. Their nomenclature for labelling these regimes, A*–G, will be used for clarity from this point forward. Regimes A* and A are both two-dimensional, whereas regime B is the onset of three-dimensionality and other regimes are all three-dimensional.

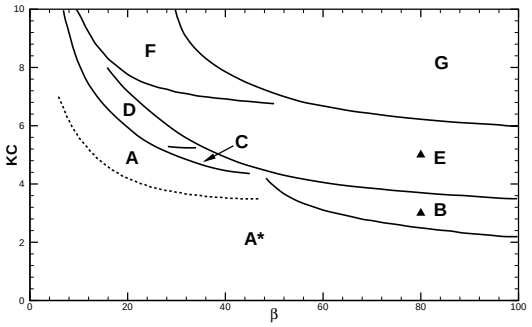

Figure 1: Map of Tatsuno & Bearman [11] identifying the different flow regimes in the KC-β plane. A: symmetric with vortex shedding, two-dimensional; A*: symmetric and attached, two-dimensional; B: longitudinal vortices, three-dimensional streaked flow; C: rearrangement of large vortices, three-dimensional; D: transverse street, three-dimensional; E: transverse street with irregular switching, three-dimensional; F: diagonal double-pair, three-dimensional; G: transverse vortex street, three-dimensional. The triangles indicate the cases discussed in this paper. The boundary between regimes A* and A was not explicitly delineated in the original diagram of [11] while in this figure, it is shown as a dashed line (see [4]).

The development of new measurement techniques that provide detailed information about the time variations of local flow properties are providing new insight into research problems. There are a large number of visualisations on low amplitude and frequency cases (for example [11]), and some other rectilinear research in quiescent flow, both experimentally or numerically. Despite this, there are few quantitative experimental investigations available especially at low values of translational amplitudes and frequencies.

The purpose of the present study is to quantitatively investigate the structure and dynamics of the flows induced by a circular cylinder performing sinusoidal oscillations in a fluid at rest for

KC<15 and β<160. A number of different flow regimes have been observed involving the generation and separation of vortices. Many of these regimes have a spatially periodic pattern, allowing the use of phase-averaging. Digital Particle Image Velocimetry (PIV) is used to yield time-resolved traces of the local velocity fields. From these measurements, phase-averaged velocity information was calculated for some cases and compared with numerical and, other experimental data. For the regimes with non-periodic pattern instantaneous velocity information was used.

Experimental Setup and Techniques

Setup

The experiments were conducted in the FLAIR free-surface closed-loop water channel in the Mechanical Engineering Department at Monash University. Experiments were performed for 3<KC<15 and 0<β<160, covering the parameter space of amplitudes and frequencies examined in [11], with one sample from each regime. The range of Re covered during the experiments is 90≤Re≤720.

The experimental model used for these experiments was a hollow circular cylinder with length of 800mm and outer diameter of 20mm, giving an aspect ratio of 40. The cylinder was made of carbon fibre tube and suspended vertically from an actuator that is controlled and moved by a micro-stepping stepper motor. This sits above the water surface with a sting connecting it to the cylinder as shown in figure 2.

A sinusoidal motion profile was used for the oscillating motion. The motion is given by

$$x(t) = A_t \cos(2\pi f_t t). \tag{4}$$

In order to achieve the different non-dimensional characteristic numbers, KC and β, three experimental parameters could be adjusted: the amplitude of oscillation of the actuator, the frequency of oscillation of the actuator and the diameter of the cylinder. For the current set of experiments, the diameter of the cylinder was kept constant, i.e. only one cylinder was used, and other parameters were adjusted accordingly.

Techniques

The flow fields around the sinusoidally oscillating circular cylinder were measured using PIV. The PIV set-up, illustrated in figure 2, was based on that originally described by [1] and developed over the past decades. The flow was seeded with round granular shaped polyamide particles having a mean diameter of 10 μm and specific gravity of 1.016. In this system, the particles were illuminated using light from two miniature Nd:YAG laser sources (Continuum Minilite II Q-Switched lasers) of a wavelength of 532nm and maximum energy output of 25 mJ pulse^{-1}. The plane of interest for these experiments was the x-y plane shown in figure 2. The thickness of the laser sheet adjusted to be approximately less than 2mm. Pairs of images were captured on a high resolution cooled CCD camera system with a maximum resolution of 4008×2672 pixels. The camera was equipped with two Nikkor (Nikon Corporation, Japan) zoom lenses of focal length of 105mm and 200mm. Eventually at a particular phase of the oscillation cycle, a number of dual images were taken over successive cycles and stored for further processing.

Each image pair was processed using in-house PIV software (see [5]). This software uses a double-frame, cross-correlation multi-window algorithm to extract a grid of velocity vectors from the PIV images. To improve the accuracy an interrogation window of 32×32 pixels was found to give satisfactory results with a 50% overlap. More than 98% of the vectors were validated in each step. This value of window corresponds to an interrogation window size of 3.12mm×3.12mm and 1.23mm×1.23mm for 105mm and 200mm lenses, respectively. With appropriate particle seeding and recursive correlation window shifting, it was possible to obtain a measurement resolution of 124×82 (total of 10168) vectors in each field. The overall field of view was 2000 pixel×1336 pixel (9.76×6.52mm and 3.84×2.56mm cylinder diameters for 105mm and 200mm lenses, respectively).

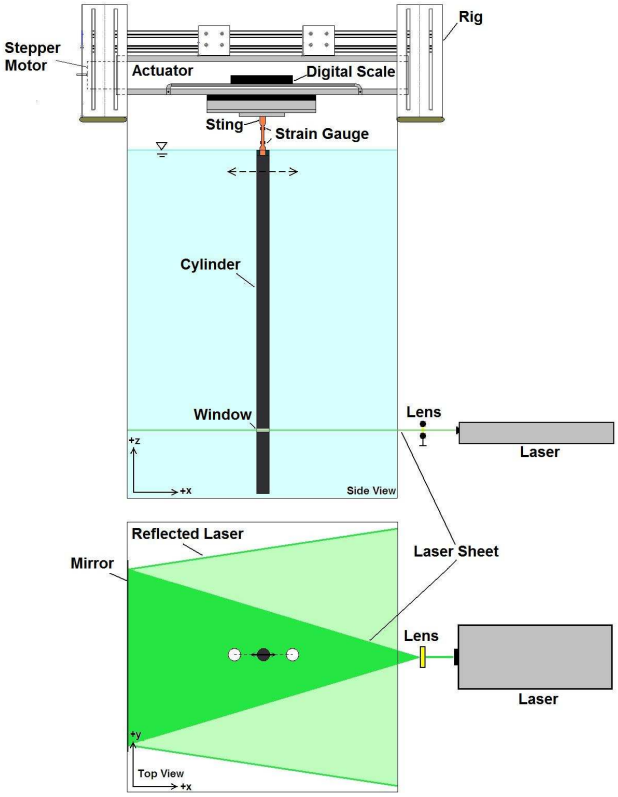

Figure 2: Overview of experimental arrangement.

A phase-locked sampling technique was applied to obtain the velocity fields at eight equispaced phases in the oscillating cycle for the highly periodic and repeatable regimes, e.g. regimes A*, A, B, D and F. The displacement fields from these analyses are presented using both instantaneous and phase-averaged vorticity fields and velocity vectors, where the phase-averaged vorticity fields and velocity vectors were calculated from the average of 30 or more instantaneous velocity fields. The two-dimensional velocity vectors obtained from the PIV processing were converted to vorticity [5] and further the circulation of vortices was calculated by integrating the vorticity in the longitudinal direction over the cross-section of the vortices in the wake at different frequencies and amplitudes of oscillation.

The velocity and spatial coordinates are non-dimensionalised by the maximum velocity of the cylinder motion, U_{max}, and the cylinder diameter, D, respectively. The vorticity is non-dimensionalised by the maximum velocity of the cylinder motion, U_{max}, and the cylinder diameter by

$$\omega_z^* = \frac{\omega_z D}{U_{max}}. \tag{5}$$

Results

Seven of the eight regimes of Tatsuno & Bearman [11] have been investigated in this study, and the results of only two of them will be presented here; regimes B (KC=3 & β=80) and E (KC=5 & β=80).

Regime B: Onset of three-dimensional instability

The structure of flow in regime B differs remarkably from that of slightly lower amplitude or lower frequency two-dimensional regimes, i.e. A* & A (refer to figure 1 for definition). Regime B is defined by Tatsuno & Bearman [11] as the onset of three-dimensional instability and longitudinal vortices. Two-dimensional vortices are not formed owing to flow separation, but a three-dimensional structure, due to an instability in the boundary-layer flow, appears near the cylinder surface [11]. Honji [6] investigated this flow in detail and named it the streaked flow. Figures 3 and 4 show this asymmetry. Figure 3 shows instantaneous spanwise velocity vectors. It is seen that the flow along the vertical axis of the cylinder is no longer uniform and varies strongly along that axis. This pattern was not seen in regimes A* and A. The cylinder shown in figure 4 is at its most right position in the oscillation cycle starting its motion from right to left. Vortices C and D, shown in figure 4, are those generated in the previous half-cycle, originating from the interaction of the flow and body. Vortices A and B have just been created and are nearly symmetrical relative to the axis of oscillation. They are more symmetrical in shape than vortices C and D which have been created and separated from the body in the previous cycle have lost planar symmetry. This asymmetry can also be seen in figure 5.

Due to the similarity in the vortex shedding pattern in regimes B, A* and A it is possible to compare these regimes together. Figure 5 shows the comparison of the same vortices for regimes B, A* and A, where non-dimensionalised peak vorticity, ω_z^*, is plotted against t/T, where T is the period of oscillation, since the vortices are grown until they are pushed away. The narrow solid line indicates the time evolution of vortex C with positive sign and the dashed line is denoting the time history evolution of vortex D with negative sign. Positive vorticity is defined as counter-clockwise rotation. The thick solid line, the average value of the non-dimensionalised peak vorticity of both vortices, is also shown for comparison purposes. Figure 5 shows that the vortices for regimes A* and A are both symmetrical and have equal peak vorticity, whereas the peak vorticity values for regime B are not symmetrical. The average values of the vorticity of both vortices, C and D, are coincident with individual values of vorticity for regimes A* and A. The asymmetry of the vorticity pattern of regime B with respect to the oscillation axis is clearly shown at t/T=0.8 in figure 5. This corresponds to the position of the cylinder in figure 4. As the absolute magnitude of vorticity of vortex C is higher than that of vortex D, the flow between these two vortices tends to tilt towards the axis of oscillation leading to asymmetry in the flow.

One of the defining characteristics of regime B is the presence of structures which vary along the span of the cylinder. In this respect this case has broken a symmetry property and is no longer considered fully two-dimensional. However, when considered in a fully three-dimensional space, the flow in regime B is clearly three-dimensional and the spanwise symmetry property of the flow has been altered from being constant along the span to having a regular variation along the span [4]. This can also be clearly seen in figure 3, which as explained shows the three-dimensionality of flow along the vertical axis of the cylinder. It is also shown that despite the onset of three-dimensionality, distribution of wavelengths along the span is periodic.

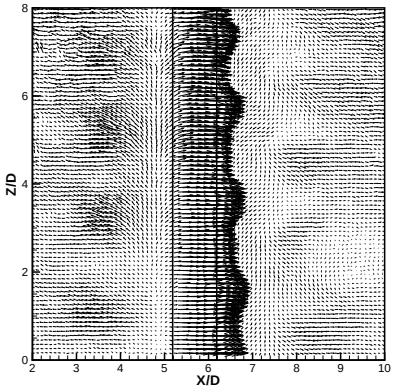

Figure 3: Instantaneous spanwise velocity vector in regime B (KC=3 & β=80), 36^{th} cycle, phase angle of 270 degrees. The cylinder is shown in the picture and is moving from right to left.

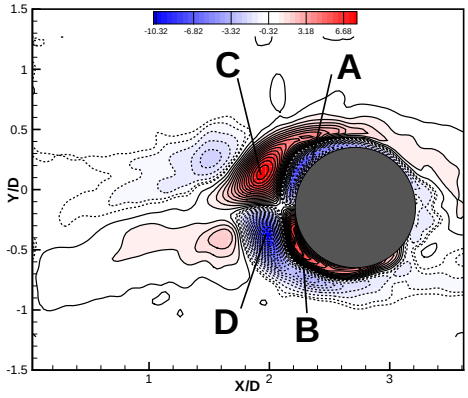

Figure 4: Pattern of phase-averaged flow structure for the sinusoidally oscillating flow past the circular cylinder in regime B (KC=3 & β=80). For dimensionless vorticity ω_z^*, $\Delta[\omega_z^*]$=0.5. The cylinder is oscillating horizontally from left to right. The cylinder is in the most right end of its motion. The results are averaged over more than 30 cycles.

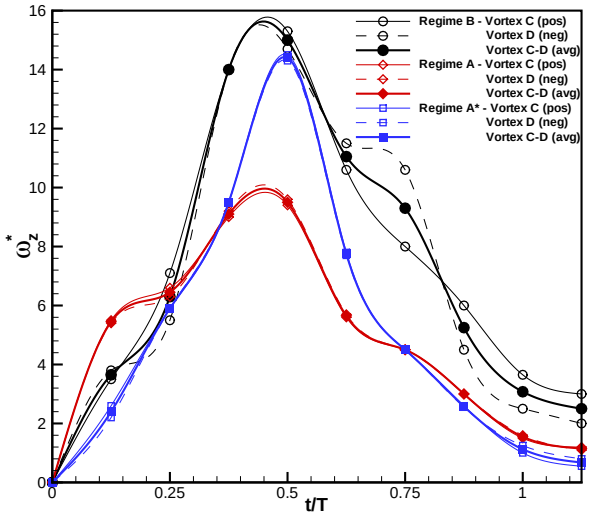

Figure 5: Comparison of time history of dimensionless peak vorticity of vortices C and D, adjacent to the cylinder body surface for regimes A*, A and B at different phase locations.

Regime E: Irregular switching of flow convection direction

According to the classification of Tatsuno & Bearman [11] the flow patterns belonging to regime E, refer to figure 1, represent temporally stable V-type vortex streets (a detailed description of this regime is given in [11]). Figure 6 shows typical examples of the behaviour of the flow in this regime, where the flow changes with time. As the flow in this regime is not phase locked the instantaneous results are presented. The instantaneous non-dimensionalised vorticity contours in figure 6 were taken in sequence during one run. According to Tatsuno & Bearman [11] the flow pattern in this regime temporarily resembles that in regime D. The flow which convects to one side of the axis of oscillation, however, intermittently changes direction to the other side. This switching of the flow occurs at irregular intervals and is presumably triggered by small disturbances. Figures 6(a) and 6(c) show temporally stable flow patterns, whereas figure 6(b) shows the transient flow changing from one side to the other. Among previous studies on flow patterns in regime E, Dütsch et al. [3] were not able to observe this intermittent change in their computational code and Iliadis & Anagnostopoulos [7] also were not able to capture this intermittent switching with their two-dimensional numerical code. Although Nehari et al. [9] have also nominally investigated regime D, and observed the switching, Elston [4] has shown that their simulation might be better categorized as being of regime E flow, rather than D. The present paper reveals the observation of the mentioned intermittent change in the direction of the V-shape vortex in regime E, which has only been observed previously on a few occasions.

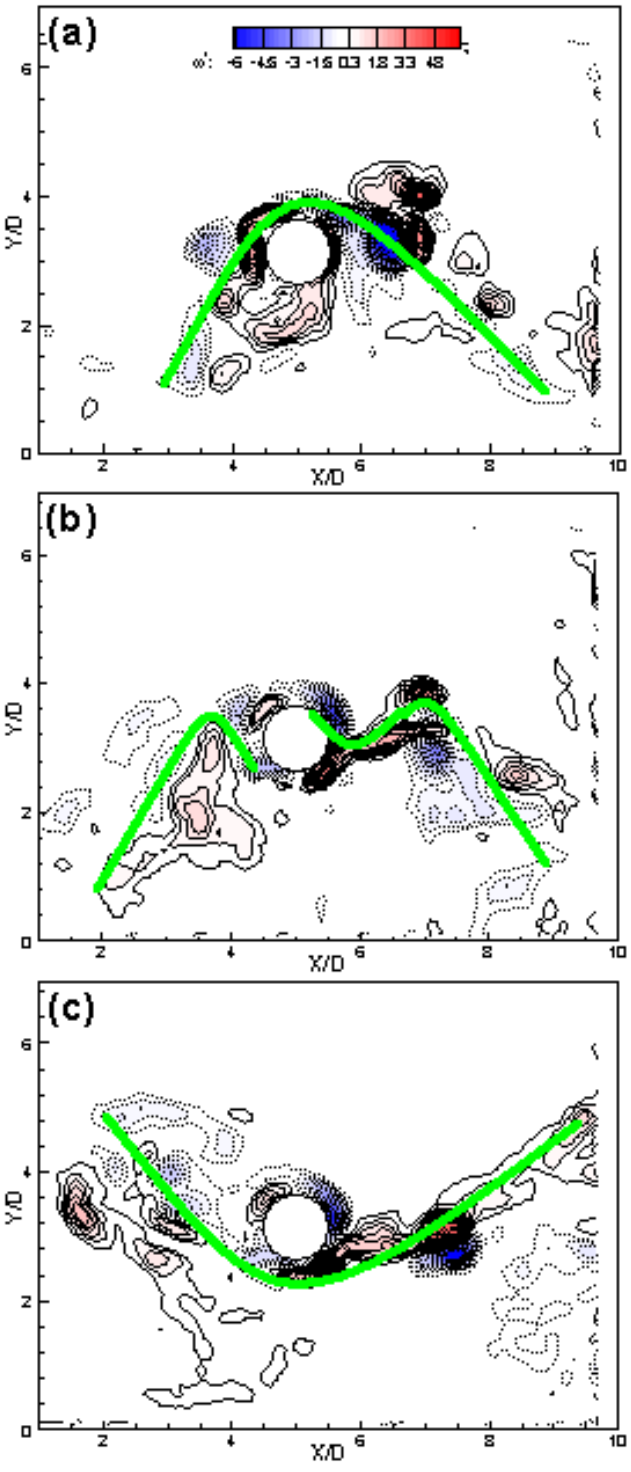

Figure 6: Patterns of instantaneous flow structure for the sinusoidally oscillating flow past the circular cylinder in regime E at KC=5 and β=80. For dimensionless vorticity ω_Z^*, $\Delta[\omega_Z^*]$=0.3. The cylinder is oscillating horizontally from left to right, at its most left position in the cycle. (a) shows cycles before change in the direction, (b) transition in the change in the direction, and (c) cycles after transition.

Conclusions

PIV has been used to quantify the flow around a sinusoidally oscillating circular cylinder in water initially at rest for the ranges of system parameters $1.6<KC<15$ and $5<\beta<160$. Three of the eight different regimes defined by Tatsuno & Bearman [11] have been described in this paper. The results for regime B, as was first discussed by [11], reveal the onset of three-dimensionality in this type of flow. The spanwise velocity vectors distribution clearly shows this feature. Contrary to the two-dimensional numerical investigations of Iliadis & Anagnostopoulos [7] and Dütsch et al. [3] and the results of Nehari et al. [9], the intermittent switching in the direction of the V-shaped vortex pattern in regime E has been observed. However, this switching was observed irregularly and its cause has not been yet determined, but as mentioned by [11] this is presumably triggered by small disturbances in the flow.

Acknowledgements

The first author would like to acknowledge the support of Monash Graduate Scholarship (MGS) and also Mechanical Engineering Department in undertaking this research.

References

[1] Adrian, R. J., Particle-imaging techniques for experimental fluid mechanics, *Annu. Rev. Fluid Mech.*, **23**, 1991, 261–304.

[2] Bearman, P. W., Graham, J. M. R., Naylor, P. and Obasaju, E. D., The role of vortices in oscillatory flow about bluff cylinders, in *International Symposium on Hydrodynamics in Ocean Engineering*, Trondheim Norway, 1981, 621–635, 621–635.

[3] Dütsch, H., Dusrt, F., Becker, S. and Lienhart, H., Low-Reynolds-number flow around an oscillating circu-

lar cylinder at low Keulegan-Carpenter numbers, *J. Fluid Mech.*, **360**, 1998, 249–271.

[4] Elston, J. R., *The structures and instabilities of flow generated by an oscillating circular cylinder*, PhD thesis, Monash University, 2005.

[5] Fouras, A. and Soria, J., Accuracy of out-of-plane vorticity measurements derived from in-plane velocity field data, *Exps. Fluids*, **25**, 1998, 409–430.

[6] Honji, H., Streaked flow around an oscillating cylinder, *J. Fluid Mech.*, **107**, 1981, 509–520.

[7] Iliadis, G. and Anagnostopoulos, G., Viscous oscillatory flow around a circular cylinder at low Keulegan-Carpenter numbers and frequency parameters, *International Journal for Numerical Methods in Fluids*, **26**, 1998, 403–442.

[8] Lin, J.-C. and Rockwell, D., Quantitative interpretation of vortices from a cylinder oscillating in quiescent fluid, *Exps. Fluids*, **23**, 1997, 99–104.

[9] Nehari, D., Armenio, V. and Ballio, F., Three-dimensional analysis of the unidirectional oscillatory flow around a circular cylinder at low Keulegan-Carpenter and β numbers, *J. Fluid Mech.*, **520**, 2004, 157–186.

[10] Stokes, G. G., On the effect of the internal friction of fluids on the motion of pendulums, *Trans. Cambridge Philos. Soc.*, **9**, 1851, 8–106.

[11] Tatsuno, M. and Bearman, P. W., A visual study of the flow around an oscillating circular cylinder at low Keulegan-Carpenter numbers and low Stokes numbers, *J. Fluid Mech.*, **211**, 1990, 157–182.

[12] Wang, C.-Y., On high-frequency oscillatory viscous flows, *J. Fluid Mech.*, **32**, 1968, 55–68.